

Photo-dynamics of polarization holographic recording in spirooxazine-doped polymer films

Shencheng Fu^a, Yichun Liu^{a,*}, Lin Dong^b, Zifeng Lu^a, Weilin Hu^c, Mingguai Xie^c

^aCenter for Advanced Optoelectronic Functional Material Research, Northeast Normal University, 5268 Renmin Street, Changchun 130024, P. R. China

^bKey Laboratory of Excited State Processes, Changchun Institute of Optics, Fine Mechanics and Physics, Chinese Academy of Sciences, 16-Dongnanhu Avenue, Changchun 130021, P. R. China

^cFaculty of Chemistry, Sichuan University, Chengdu, 610064, P. R. China

Received 16 September 2004; received in revised form 18 December 2004; accepted 4 January 2005

Available online 2 February 2005

Abstract

Polarization holographic gratings were recorded in 6-cyano-1,3,3-trimethylspiro[indolino-2,3-[3H]naphtha-[2,1-b][1,4]oxazine] (SO-1)-doped PMMA films. A photochemical equilibrium was observed in holographic gratings recorded by (s,s) polarized He–Ne beams with accompanying UV irradiation. For comparison, (s,p) polarization holographic recordings were also performed. The observed maximum value of the diffraction efficiency of (s,s) gratings was higher than that of (s,p) gratings. The mechanism of the photo-dynamics of the two polarization holographic recordings for SO-1 was investigated in detail.

© 2005 Elsevier B.V. All rights reserved.

PACS: 42.70.Ln; 78.20.Wc

Keywords: Polarization holography; Spirooxazine; He–Ne laser; UV-light irradiation

1. Introduction

Spirooxazines (SOs) and spiropyranes (SPs) represent an important class of photochromic compounds [1–7]. In contrast with spiropyranes, SOs exhibit high light stability and fatigue resistance [8,9], which provide the possibility of practical applications in lenses of variable optical density, displays, filters, and optical-storage devices. Photochromism in SOs and SPs arises from carbon-oxygen (C_{spiro}–O) bond cleavage in the colorless spiro form upon UV-light excitation and subsequent isomerization to colored open forms, called photomerocyanines (PMCs). PMCs can revert to the spiro forms thermally or photochemically. Hence, it is possible to perform holographic recording with visible light for SOs pre-irradiated by UV-light. Previously, most studies of SOs focused on photochromism and optical storage employing UV, Ar⁺, or CO₂ lasers as the writing beams [10–

12]. Recently, photo-induced birefringence and polarization holographic recording for spirooxazines was accomplished with red light [13]. However, little is known about the photodynamic mechanism of polarization holographic recording for SOs.

In this work, polarization holographic recording for 6-cyano-1,3,3-trimethylspiro[indolino-2,3'-[3H]naphtha-[2,1-b][1,4]oxazine] (SO-1) doped PMMA films irradiated by UV-light was accomplished by 632.8 nm He–Ne laser light. The mechanism of the photo-dynamics of polarization holographic recording for SO-1 was investigated in detail.

2. Experiment

2.1. Materials and preparation

The chemical structures of 6-cyano-1,3,3-trimethylspiro[indolino-2,3-[3H]naphtha-[2,1-b][1,4]oxazine] (SO-1) and the corresponding UV-induced photomerocyanine (PMC)

* Corresponding author. Tel.: +86 431 5099168; fax: +86 431 5684009.

E-mail address: yeliu@nenu.edu.cn (Y. Liu).

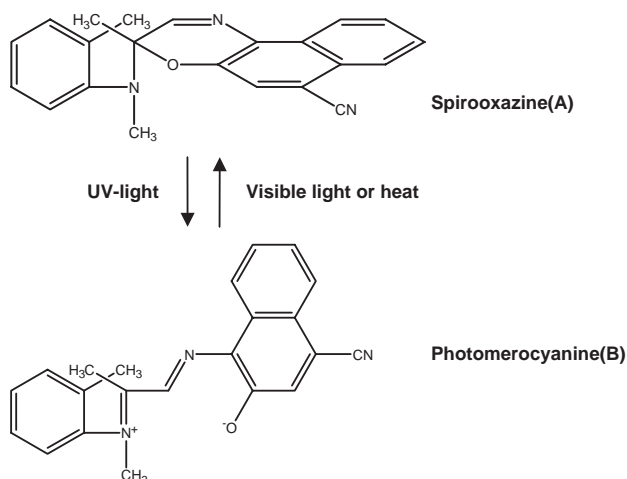


Fig. 1. Chemical structure of SO-1 and corresponding UV-induced PMC form.

are shown in Fig. 1. SO-1 was synthesized with microwave irradiation [14]. Commercially available poly(methyl methacrylate) (PMMA) was used without further purification. Both SO-1 and PMMA were dissolved in CHCl_3 and then cast on a clean glass substrate. After solvent evaporation, the resulting composite film was used for the measurement of polarization holographic recording. The pre-set dye concentration was 10 wt.%, and typical film thickness was $10 \pm 1 \mu\text{m}$, as measured with a Precision Ellipsometer.

2.2. UV-Vis measurements

Fig. 2 shows the UV-Vis spectra of PMMA films containing SO-1(a) and PMC(c), obtained with a Perkin-Elmer Lambda 900 spectrophotometer over the range of 190–3200 nm. The absorption bands at 365 nm correspond to $\pi-\pi^*$ electronic transition for both SO-1 and PMC, while the absorption near 633 nm corresponds to $n-\pi^*$ electronic transition and intermolecular charge-transfer of PMC [15]. For comparison, the UV-Vis spectrum of SO-1 in dilute solution is also shown (b). The absorption maximum ($\lambda_{\text{max}}=650 \text{ nm}$) in the visible wavelength of the PMC-doped PMMA film is red-shifted by 86 nm relative to that in

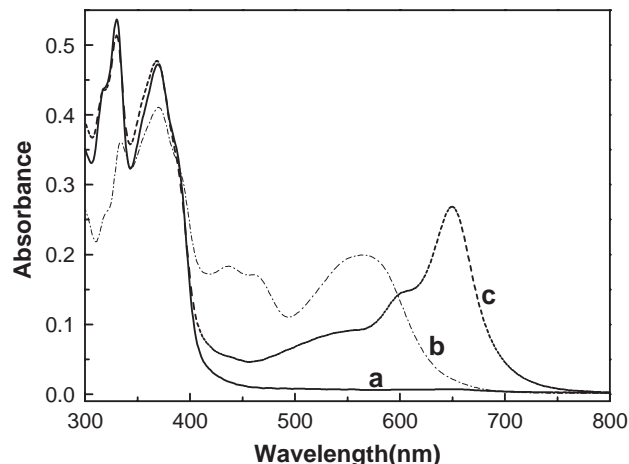


Fig. 2. UV-Vis spectrum of PMMA film doped with 10 wt.% SO-1 (a), the corresponding spectrum after UV-induced isomerization of SO-1 to PMC (b), and the spectrum of SO-1 doped in CHCl_3 after UV irradiation with the concentration of 0.01 mg/ml (c).

dilute solution (564 nm), indicating a very strong J-aggregation of PMC molecules in the polymer films [16].

2.3. Optical setup

Holographic recording measurements were made possible by two interferential laser beams irradiating the sample, as shown in Fig. 3. The major elements of the experimental setup were as follows. A linearly polarized He-Ne laser (632.8 nm) generated the writing and reading beams. A half-wave plate was used to rotate the polarization of the He-Ne beam. The diameter of the laser beams was $\sim 0.3 \text{ cm}$, and the intersecting angle between the beams was $\sim 10^\circ$. A mercury-arc lamp (125 mW) was used to irradiate the sample with homogenous, incoherent light at 365 nm ($\sim 1 \text{ mW/cm}^2$ at the sample location). The diffractive signals were registered on a CCD camera interfaced with a computer.

3. Results and discussion

Fig. 4 shows time evolution of the first-order diffractive signal of the holographic gratings generated by two He-Ne

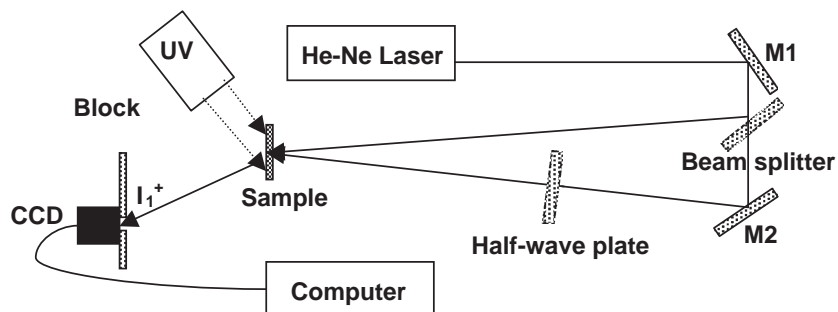


Fig. 3. Experimental configuration for the recording of holographic gratings by two He-Ne laser beams, where M denotes a mirror, P a polarizer, CCD a charge coupled device (sensitive region from 350 to 900 nm).

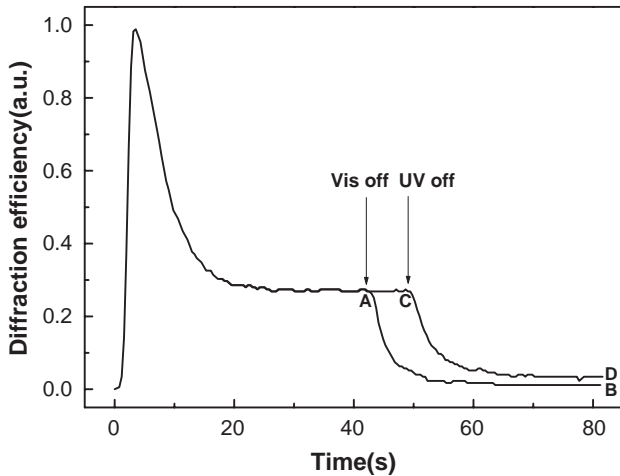


Fig. 4. The first-order diffractive signal of the holographic gratings pre-irradiated by UV-light versus time. “On” means UV-light or visible light (He–Ne laser beam) is turned on and “off” means UV-light is turned off.

laser beams with the same (s,s) polarizations. The power density of each beam was $10/0.07 \text{ mW/cm}^2$. The overall change in the diffractive signal is normalized between 0 and 1, for clarity of presentation. The experimental sequences are described as follows: first, the film was exposed to UV irradiation until maximal coloring was observed. Then, as illustrated in Fig. 4, with the UV source on, the two linearly polarized He–Ne beams irradiated the sample and the diffraction intensity increased rapidly to a maximum value in a few seconds and then decreased gradually to a fix value (point A). When one He–Ne beam was switched off, with the UV source on, the diffractive-signal intensity decreased further, approaching a constant value at point B. Alternatively, when the UV source was turned off at point C, and the He–Ne beams remained on, the measured diffractive-signal intensity decreased gradually to point D.

Some SO-1 molecules are transformed to PMC molecules after UV pre-irradiation, competing with thermal effects. Fig. 5a indicates that the interference pattern of (s,s) polarization contains components of both isomerization and orientation. Hence, the initial diffraction maximum is attributed mainly to the isomerization of PMC to SO-1 upon irradiation by the linearly polarized He–Ne beams and PMC orientation perpendicular to the direction of He–Ne polarization. However, incoherent UV-light not only drives the competing reverse reaction of SO-1 to PMC, but also randomizes the orientation of PMC molecules. Eventually, chemical species equilibrium between SO-1 and PMC and reorientation equilibrium for PMC molecules are reached at point A in Fig. 4. When only one He–Ne beam is switched off at point A, the interferential pattern of (s,s) polarization disappears gradually and the value of diffraction efficiency tends to zero (point B). Alternately, when UV-light is turned off at point C, PMC is transformed to SO-1 thermally and the interference pattern of (s,s) polarization is also destroyed, and the diffractive signal falls gradually to point D. The non-zero value at point D is attributed to residual

PMC molecules trapped in the PMMA matrix. As for the interference pattern of (s,p) polarization, the resulting light field is not modulated in intensity, but a similar pattern of information is created by means of the polarization states which are modulated consequently to the optical path difference [17], as shown in Fig. 5b. Numbers on the top of the graphs indicate phase shift between the two incident waves [18].

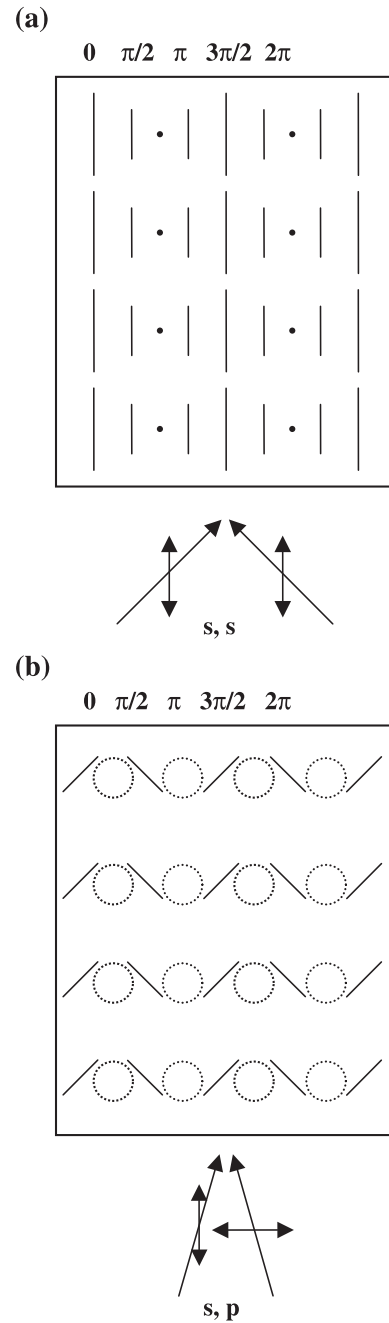


Fig. 5. The interference patterns obtained for (s,s) (a, by Shencheng et al.) and (s,p) (b, by Shencheng et al.) polarization configurations of the incident beams. Numbers on the top of the graphs are relative to the phase shift between the two incident waves [18].

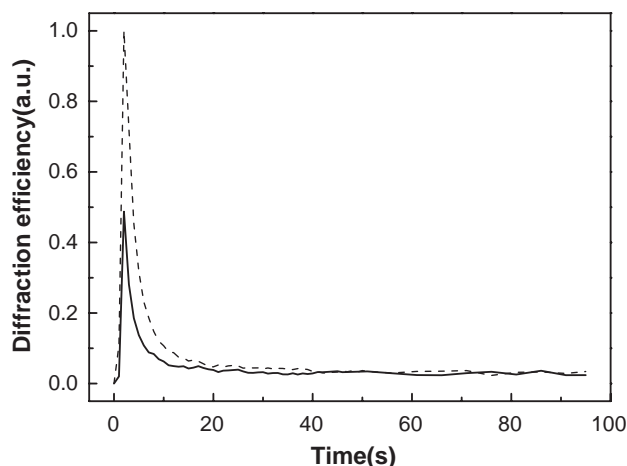


Fig. 6. The first-order diffractive signal of the holographic gratings pre-irradiated by UV-light versus time with the same (s,s) polarization or different (s,p) polarization (dotted line and solid line, respectively).

To further investigate the photodynamics mechanism of polarization holographic recording for SO-1, the effect of UV-light was eliminated during polarization holographic recording. The sample was initially exposed to the UV excitation beam, until maximal coloring occurred, then separately exposed to two parallel or orthogonal polarized He–Ne beams (632.8 nm) of 10 mW. Fig. 6 shows time evolution of the first-order diffractive signals of the holographic gratings when recorded with (s,s) and (s,p) polarizations as dotted and solid curves, respectively. Upon turning on the He–Ne laser, the diffractive signals of both (s,s) and (s,p) gratings rapidly reached a maximum value, and then dropped almost to zero. The maximum value of the diffraction efficiency of (s,s) gratings was higher than that of (s,p) gratings. For (s,s) gratings, the interference pattern is formed by both the isomerization from PMC to SO-1 and the orientation of PMC molecules, which results in the formation of isomerization and orientation gratings. With the competition of the two gratings, the interference pattern of (s,s) gratings reaches the optimal amplitude and structure rapidly, with the isomerization contribution initially dominant. However, as PMC molecules are transformed to SO-1 molecules by He–Ne laser and thermal effects, the interference pattern degrades rapidly. PMC has an extremely large dipole moment because of its ionic form, while the dipole moment of SO-1 is relatively small [19–21]. Hence, the orientation of SO-1 is neglected and the interference pattern of (s,p) polarization is considered to arise solely from the orientation of PMC molecules. On turning on He–Ne laser, orientation gratings are recorded and the value of the (s,p) diffraction efficiency reaches maximum value rapidly. With time, He–Ne light and thermal effects drive PMC to SO-1 with random orientation, and the diffraction efficiency drops almost to zero after approximately 30 s.

The hologram can be rewritten and the same value of diffraction efficiency can be achieved after multiple uses.

4. Conclusion

Polarization holographic gratings of 6-cyano-1,3,3-trimethylspiro[indolino-2,3-[3H]naphtha-[2,1-*b*][1,4]oxazine] pre-irradiated by UV-light were recorded by He–Ne laser of 632.8nm. The maximum value of the diffraction efficiency of (s,s) gratings is higher than that of (s,p) gratings. The mechanism of the photo-dynamics of polarization holographic recording for SO-1 was investigated in detail. The spirooxazine-doped polymer film allowed multiple uses without apparent fatigue.

Acknowledgements

This work was supported by the National Natural Science Foundation of China (60176003), the Foundational Excellent Researcher to Go beyond Century of Ministry of Education of China, and Science Foundation for Young Teachers of Northeast Normal University.

References

- [1] G. Berkovic, V. Krongauz, V. Weiss, *Chem. Rev.* 100 (2000) 1741.
- [2] Roni A. Kopelman, Sean M. Snyder, Natia L. Frank, *J. Am. Chem. Soc.* 125 (2003) 13684.
- [3] V.M. Anisimov, S.M. Aldoshin, *Theor. Chem.* 419 (1997) 77.
- [4] K. Sasaki, T. Nagamura, *Appl. Phys. Lett.* 71 (1997) 4.
- [5] L. Hou, H. Schmidt, *Mater. Lett.* 27 (1996) 215.
- [6] V.S. Marevsev, N.L. Zaichenko, *J. Photochem. Photobiol., A* 104 (1997) 197.
- [7] A.K. Chibisov, H. Gomer, *J. Phys. Chem.* 103 (1999) 5211.
- [8] N.Y.C. Chu, *Can. J. Chem.* 61 (1983) 300.
- [9] U.W. Grummt, M. Reichenbacher, R. Paetzold, *Tetrahedron Lett.* 22 (1981) 3945.
- [10] V. Weiss, V.A. Krongauz, *J. Phys. Chem.* 98 (1994) 7562.
- [11] V. Weiss, A.A. Friesem, V.A. Krongauz, *Opt. Lett.* 18 (1993) 1089.
- [12] T. Izawa, M. Kamiyama, *Appl. Phys. Lett.* 71 (1969) 4.
- [13] S. Fu, Y. Liu, Z. Lu, L. Dong, W. Hu, M. Xie, *Opt. Commun.* 242 (2004) 115.
- [14] W. Hu, Q. Jiang, K. Zou, Y. Huang, M. Xie, *Chem. Res. Appl.* 15 (2003) 282.
- [15] G.H. Brown, *Photochromism*, Wiley, New York, 1971.
- [16] H. Menzel, B. Weichart, A. Schmidt, S. Paul, W. Knoll, J. Stumpe, *T. Fischer, Langmuir* 10 (1994) 1926.
- [17] T. Todorov, L. Nikolava, N. Tomova, *Appl. Opt.* 23 (1984) 4309.
- [18] P.-A. Blanche, Ph.C. Lemaire, C. Maertens, P. Dubois, R. Jerome, *Opt. Commun.* 185 (2000) 1.
- [19] S. Hosotte, M. Dumont, *Synth. Mater.* 81 (1996) 125.
- [20] D.J. Williams, *Angew. Chem., Int. Ed. Engl.* 23 (1984) 690.
- [21] A. Dulcis, C. Flytzanis, *Opt. Commun.* 25 (1978) 402.